

# CALCULATION OF ZETA-POTENTIALS FROM ELECTROKINETIC DATA

C

Nikos Spanos

Pavlos G. Klepetsanis

Petros G. Koutsoukos

*Institute of Chemical Engineering and High Temperature Chemical Process, Patras, Greece*

## INTRODUCTION

Electrokinetic phenomena are called processes in which a charged surface (or colloidal charged particle) is set in a relative motion with respect to the adjacent polar liquid phase. Thus, the application of external electric field causes the movement of charged particles or liquid near to a charged surface and the movement of charged particles or liquid near to charged surface causes the appearance of electric potential. The most familiar electrokinetic phenomena are electro-osmosis, streaming potential, electrophoresis, and sedimentation potential (1).

In electro-osmosis, when an external electric field is applied on an immobile capillary, with charged walls, flow of the liquid inside it is observed. The streaming potential appears when a pressure drop pushes the liquid to flow through an immobile capillary with charged walls or through a porous plug. In electrophoresis, the charged particles move in a stationary liquid medium when an external electric field is applied, and the sedimentation potential is established when charged particles are moving relative to stationary liquid under the action of gravity. The electrophoresis and sedimentation potentials are closely linked phenomena. A brief description of the above-mentioned electrokinetic phenomena is given in Table 1.

All electrokinetic phenomena are related to the development of electrical double layer at the particle/electrolyte interface. The zeta potential,  $\zeta$ , is the most important parameter of electrical double layer, which can be determined from the electrokinetic measurements. The  $\zeta$  potential is defined as the potential of shear plane of the particle when it moves in liquid.

## ELECTROPHORESIS

### Introduction

The most popular method for the determination of zeta potential is the particle microelectrophoresis. The term “particle microelectrophoresis” is used to distinguish the method for the determination of zeta potential from other electrophoresis methods used for the separation of proteins and other charged compounds. In this method, an external electric field is applied across the sample, and the charged particles move toward the oppositely charged electrode. A dc device is used for voltage application. The particle velocity is strongly dependent on its surface charge. In particle electrophoresis, the objective is to measure the particle velocity in a known electric field. The measured quantity is the electrophoretic mobility,  $u$ , which is given by the following equation:

$$u = \frac{v}{E} \quad (1)$$

where  $v$  is the particle velocity and  $E$  is the strength of the applied electric field. The electrophoretic mobility is measured in  $\text{ms}^{-1}/\text{Vm}$  in SI units.

### Instrumentation

The standard electrophoresis cell usually consists of a horizontal capillary tube of either circular or rectangular cross section, with an electrode at each end and suitable inlet and outlet connections for cleaning and filling. The tube is made from quartz, for chemical inertness and for optical reasons. The internal diameter for circular cross-section tube is usually 4 mm, and its length must be 10

**Table 1** Summary description of the most familiar electrokinetic phenomena

Electrokinetic phenomenon	Driving force	Resulting phenomenon	Moving phase	Stationary phase	Quantity measured	Symbols	SI units
Electrophoresis	Electric field	Particle movement	Particles	Liquid	Electrophoretic mobility	$u$	$\text{m}^2 \text{V}^{-1} \text{s}^{-1}$
Sedimentation potential	Particle movement	Electric field	Particles	Liquid	Potential difference per unit of length	$E_{\text{sed}}/l$	$\text{V m}^{-1}$
Electroosmosis	Electric field	Pressure gradient	Liquid	Plug or capillary	Electro-osmotic volume flow per unit current	$V_{eo}/I$	$\text{m}^3 \text{C}^{-1}$
Streaming potential	Pressure gradient	Electric field	Liquid	Plug or capillary	Streaming potential (or current) per unit of the applied pressure	$E_s/P$ (or $I_s/P$ )	$\text{V m}^2 \text{N}^{-1}$ (or $\text{C m}^2 \text{N}^{-1} \text{s}^{-1}$ )

times its diameter. The large surface area of the capillary makes it relatively easy to thermostat the sample. The capillary has a disadvantage that its length limits the size of the electric field that can be applied (especially for low-conductivity samples). The small cross section of the capillary limits the current that can flow. Any Joule heating in salty and conductive media is thus avoided. The electrodes are made from black platinum or palladium to avoid gas evolution and are mounted coaxial in with the measurement capillary tube and in contact with the sample. During the measurements, the cell is closed with an electric valve (1, 2).

Electrophoretic measurements are complicated by the simultaneous appearance of electro-osmosis. The internal glass or quartz surfaces of the cell are usually charged. As a result, the liquid flows in the cell when a voltage is applied across the electrodes. The flow occurs in one direction close to the wall and in the opposite direction in the center of the tube. This results in a parabolic distribution of the fluid velocity with depth, and the true electrophoretic velocity is only observed at locations in the tube where the electro-osmotic flow and return flow of the liquid cancel (stationary layers). For a cylindrical cell, the stationary layers are located at distances equal to 14.62% of the internal diameter from each cell wall. For a flat cell, the stationary layers are located at about 20 and 80% of the total depth, the exact locations depending on the width/depth ratio.

The first method used for the measurement of electrophoretic mobility is the ultramicroscope method (1, 2). In this method, white light illumination is used, and the particle motion is observed with a microscope at 90° to the incident light direction. When viewed through the microscope, the suspended particles appear as pin-points of light. When the field is applied, all particles of the same depth move with essentially the same velocity. The velocity is measured by timing individual particles mi-

grating between two well-defined points in the eyepiece graticule. The applied voltage is adjusted to give timings of about 10 s. Faster times introduce timing errors, and slower times increase the error from the Brownian motion. Also, the value of the applied voltage is related to the suspension conductivity. As conductivity increases, the voltage decreases to avoid heating of the suspension. The temperature increase of suspension leads to increased Brownian movement. The electrophoretic velocity measured divided by the applied electric field yields the electrophoretic mobility,  $u$ .

The ultramicroscope method suffers from several serious disadvantages. The most important disadvantages of the microscope method include the following:

1. This method is very slow, tedious, and time-consuming.
2. Only a few particles can be followed and timed; thus, the method yields results of low statistical significance and cannot be used to determine mobility distributions or separate multimodal mobility distributions (the suspensions are usually polydisperse).
3. The method is confined to particles visible under microscope (in practice  $\geq 0.5$  micron).
4. The method is straining the operator's eyes.

These disadvantages have severely limited the use of this method despite instrumental developments done to solve some of the problems [rotating prism and use of monitor to measure particle velocity (3)].

A more sophisticated method is presently used for the measurement of electrophoretic mobility. This method uses a low-power laser to produce light that is not just bright but coherent, the Photon Correlation Spectroscopy (PCS) technique and fast computers connected with digital correlators for signal analysis. A large number of instruments dedicated to the measurement of electrophor-

etic mobility using this method are now available in the market. Particle microelectrophoresis has thus been transformed from a difficult, tedious technique requiring skill on the part of the operator to one, that can be successfully applied routinely to give fast, accurate data without extensive practice or training.

In Fig. 1, a schematic layout of a modern instrument, for the measurement of electrophoretic mobility, based on PCS is shown. The light beam from a low-power He–Ne laser is split into two beams with a beam splitter: One reflects off a moving mirror (modulator) and the other off a plain mirror, and they cross again in the sample tube at the stationary layer (4). The intersection point of two beams is set automatically at the stationary layer. At the intersection of the two beams, a pattern of interference fringes is formed. Particles moving across the fringes under the influence of the applied electric field scatter light, the intensity of which fluctuates with a frequency that is related to their velocity. The signals resulting from the individual photons of scattered light detected by the fast photomultiplier are fed to a digital correlator, and the resulting correlation function is analyzed to determine the frequency spectrum. From this, the mobility spectrum and hence the zeta potential are calculated and displayed.

The complete measurement takes only a few seconds, but, more important, it is made over a sample of many millions of particles, something impossible to be done with an ultramicroscope method. It therefore represents a comprehensive and accurate assessment of the entire sample and the mobility spectrum of all of the suspended

particles. Furthermore, the sensitivity is sufficient that particles as small as 50 nm and up to several microns can be measured.

The sign of the mobility is determined by causing one of the mirrors to oscillate backward and forward. This causes the fringe pattern to oscillate with a known frequency. The observed Doppler frequency of the light scattered by particles moving through the fringes can thus be measured by reference to the applied modulation frequency and will be either higher or lower than the applied frequency, depending upon the direction of movement. The modulation frequency is greater than any shift in frequency that could result from electrophoretic motion of the particles. The determination is thus unequivocal.

A further substantial benefit of this use of an imposed base frequency is that particles with very low or zero charge that would otherwise produce very tiny Doppler shifts now give rise to substantial signals that can be measured with high accuracy.

In the electrophoresis cell of modern instruments, there are four electrical connections: Two of these connect the driving field, and two are sensing electrodes to measure the true field, because it is not possible to obtain it from the driving voltage because of the electrode polarization losses (5). Moreover, through the use of an improved power supply, voltages from 0 to 400V can be applied with the ability for dc and ac operation. The ability to stabilize either the voltage or the current is advantageous. Current stabilization is effective in very conductive samples, because mobility and conductivity track are inter-

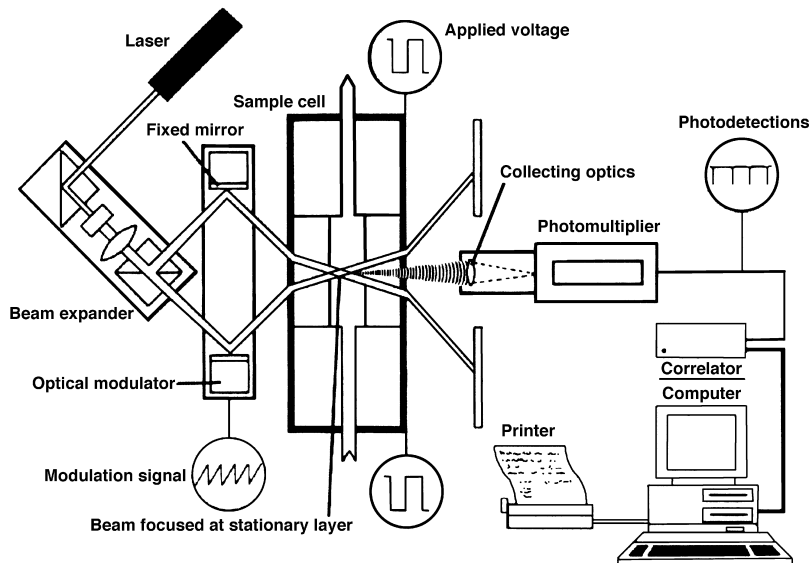


**Fig. 1** Schematic arrangement of Photon Correlation Spectroscopy microelectrophoresis instrument.

related, and cell heating will give rise to an increase in conductivity. The applied ac voltage has square waveform, with a gap between successive applications of power, to avoid gas evolution at the electrodes. The frequency of applied electric field is usually 2 Hz.

### Calculation of Zeta Potential from Electrophoretic Mobility Measurements

Even though the measurement of electrophoretic mobility is relatively easy with the new technique, its interpretation is more difficult. Henry derived a general equation for the calculation of zeta potential from electrophoretic mobility, for conducting and nonconducting spheres (1, 2). This equation is given by Eq. 2.

$$\zeta = \frac{3\eta u}{2\epsilon_0\epsilon[1 + \lambda f(\kappa\alpha)]} \quad (2)$$

where  $f(\kappa\alpha)$  varies between zero for small values of  $\kappa\alpha$  and 1.0 for large values of  $\kappa\alpha$ , and the parameter  $\lambda$  is a function of the conductivity of the bulk electrolyte solution,  $K^L$ , and the particle conductivity,  $K^S$ , and is given by the following equation:

$$\lambda = \frac{K^L - K^S}{2K^L - K^S} \quad (3)$$

For small values of  $\kappa\alpha$ , the effect of particle conductance is negligible. For large values of  $\kappa\alpha$ , the Henry equation predicts that  $\lambda$  should approach -1, and the electrophoretic mobility approaches zero as the particle conductivity increases.

For nonconducting particles ( $\lambda = 1/2$ ), the Henry equation can be written in the form:

$$\zeta = \frac{3\eta u}{2\epsilon_0\epsilon f(\kappa\alpha)} \quad (4)$$

where  $\eta$  is the viscosity of the medium,  $\epsilon_0$  is the permittivity of free space, and  $\epsilon$  is the relative permittivity of the medium.  $\kappa\alpha$  is the product of the Debye parameter ( $\kappa$ ) and the particle radius  $\alpha$ . The value of  $\kappa$  can be calculated from the expression:

$$\kappa = \left( \frac{2000e^2 N_A}{\epsilon_0 \epsilon k T} I \right)^{1/2} \quad (5)$$

in which  $e$  is the electronic charge,  $k$  is the Boltzmann's constant,  $N_A$  is the Avogardo's constant,  $T$  is the tem-

perature, and  $I$  is the solution ionic strength. The ionic strength of the solution in mol/L can be calculated from:

$$I = 0.5 \sum c_i z_i^2 \quad (6)$$

where  $c_i$  is the concentration of the particular ionic species and  $z_i$  is the respective valency.

The thickness of the ionic atmosphere at the particle surface is strongly dependent on the aqueous medium ionic strength. The reciprocal of the Debye parameter ( $1/\kappa$ ) is generally taken as a measure of the thickness of the electrical double layer. The charged region around a particle extends to about  $3/\kappa$  before the potential falls below 2% of its value at the surface. For ionic strength equal to 0.01 M, the  $3/\kappa$  is about 10 nm, while for ionic strength equal to  $10^{-5}$  M, it is about 280 nm (5).

The Henry function  $f(\kappa\alpha)$  has two limiting values for nonconducting particles:

1. If the particle is large and the double layer thin, then  $\kappa\alpha \gg 1$ , and the zeta potential is given by the Smoluchowski equation:

$$\zeta = \frac{\eta u}{\epsilon_0 \epsilon} \quad (7)$$

2. If the particle is small with extended double layer, then  $\kappa\alpha \ll 1$ , and the zeta potential is given by the Henry equation:

$$\zeta = \frac{3\eta u}{2\epsilon_0\epsilon} \quad (8)$$

If  $\kappa\alpha$  is around 1, then the expression for the calculation of zeta potential is more complicated.

The Henry equation is based on the following assumptions (1):

1. The Debye-Hückel approximation is used.
2. The loss of double-layer symmetry during the movement of particle (relaxation effect) and the abnormal surface conductance in the vicinity of the charged surface (surface conductance) are not taken account.
3. The parameters  $\epsilon$  and  $\eta$  are assumed to be constant throughout the mobile part of the double layer.

A large number of effects significantly influence the movement of charged particles in the microelectrophoresis cell (6). When the external electric field is applied, the ions in the mobile part of the double layer show a net movement in a direction opposite to that of the particle. This creates a local movement of liquid, which opposes the

motion of the particle and is known as electrophoretic retardation. The reduction of electrophoretic mobility is often by one or more orders of magnitude. The Henry equation takes into account the electrophoretic retardation.

The movement of the particles relative to the mobile part of the double layer results in double-layer distortion, because a finite time (relaxation time) is required for the original symmetry to be restored by diffusion and conduction. The resulting asymmetric mobile part of the double layer exerts a retarding force on the particle, known as the relaxation effect. Relaxation can be neglected when  $\kappa\alpha$  is either small ( $< 0.1$ ) or large ( $> 300$ ). It is, however, significant for intermediate  $\kappa\alpha$  values, especially at high potentials and when the counterions are of high charge number and/or have low mobilities. The reduction of particle electrophoretic mobility by the relaxation effect is usually not as large as the electrophoretic retardation. A reduction of the mobility by 10 to 50% is usual, but is not accounted for in the Henry equation.

The distribution of ions in the diffuse part of the double layer gives rise to conductivity in this region, which is in excess of that in the bulk solution. Surface conductance will affect the distribution of the electric field near the surface of a charged particle and its electrokinetic behavior. The effect of surface conductance on electrokinetic mobility can be neglected when  $\kappa\alpha$  is small, because the applied electric field is not significantly affected by the particle. When  $\kappa\alpha$  is not small, calculated zeta potentials may be significantly low, due to surface conductance.

Dukhin and Derjaguin (7) have taken into account the relaxation effects and surface conductivity in their polarized double layer model. In this model, the zeta potential can be calculated from the electrophoretic mobility using the equation:

$$\zeta = \frac{\eta u A (1 + 2\text{Rel})}{\varepsilon_0 \varepsilon [(1 + \text{Rel})A - \text{Rel} \ln(\cos hA)]} \quad (9)$$

where  $\text{Rel} = e^{|\bar{\psi}_d|/2}/\kappa\alpha$ ,  $A = z|\bar{\zeta}|/4$ ,  $\bar{\zeta} = e\zeta/kT$  (dimensionless zeta potential),  $\bar{\psi}_d = \psi_d/kT$ , and  $\psi_d$  is the Stern potential. The relaxation parameter, Rel, is introduced as a measure of the effect both of surface conductivity and double layer relaxation on the electrophoretic mobility of strongly charged particles. The above Eq. 9 was derived assuming equal valency and mobility of the counter and co-ions. The comparison with the exact numerical calculations showed that the previous equation is rather accurate for  $\kappa\alpha > 30$  and arbitrary zeta potential. Another explicit formula of high accuracy [ $< 1\%$  for

arbitrary zeta potential and wider range of application ( $\kappa\alpha > 10$ )] has been suggested (8, 9).

## C

### Application of Zeta Potential

The major area of application of colloid-electrolyte phenomena is to understand stability and flocculation effects. The DLVO (Deryaguin-Landau-Verwey-Overbeek) theory states that the stability of the colloids is a balance between the attractive Van der Waals forces and the electrical repulsion due to the surface charge. The magnitude of the zeta potential gives an indication of the potential stability of the colloidal systems. In general, if all particles of a suspension have a large negative or positive zeta potential, they will repel each other, and there is dispersion stability. If the zeta potential falls below a certain level, the colloid will aggregate due to the attractive forces. A dividing line between stable and unstable aqueous dispersions is generally taken at absolute zeta potential of 30 mV.

There are two main areas where zeta potential is important in the pharmaceutical industry: emulsion stability and suspension stability (10).

Triglyceride emulsions are medical products. They are submicron emulsions of vegetable oils in water, emulsified by phospholipids that provide a high zeta potential ( $-40$  to  $-50$ mV at  $\text{pH} = 7$ ) and a correspondingly long shelf life (2 to 3 years). The emulsions are used to feed patients intravenously who cannot be fed orally. Such patients also need other nutrients, including amino acids, glucose, and electrolytes. In such mixture, there is a wide scope for interaction between the components, and in many mixtures, the fat emulsion becomes unstable and coalesces or flocculates in a few days. In this condition, it is unsuitable for infusion, and so the mixtures are normally made up just before administration, using sterile techniques. An understanding of the stability of the emulsion in these systems would be helpful in predicting which mixtures would be unstable and possibly in producing stable mixtures with long shelf lives. Also, emulsions have been used as drug delivery systems, and, in many cases, an understanding of the electrophoretic behavior is crucial in formulation design (flocculation).

Liposome suspensions are used increasingly as drug targeting and delivery systems. Liposomes are formed when a phospholipid is dispersed in water. They can vary in size from a few tens of nanometers to several microns, depending on how they are made, and their surface chemistry is dependent on the nature of phospholipids used to produce them. Many earlier studies classified liposomes as neutral, acidic, and basic. The neutral liposomes were made from phosphatidylcholine, the acidic ones had added acidic lipids (as phosphatidylserine), and the basic had

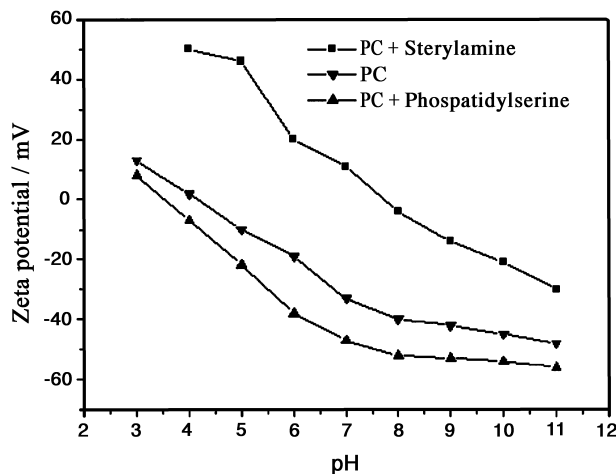


**Fig. 2** Effect of pH on  $\zeta$ -potential of liposomes with different phospholipid composition.

added sterylamine. In Fig. 2, the zeta potential of three such liposomal systems is shown as a function of pH. Also, the effect of various drugs and ions in the stability of liposome suspensions can be studied with the particle microelectrophoresis method.

## ELECTROOSMOSIS

Electroosmosis is the movement of a liquid through a capillary, membrane, or porous plug of material usually made up of granules with a particle size of the order of micrometers or submicrometers, as a consequence of an applied electric field. Provided that the walls of the capillary and the surface of the membrane or of the particles constituting the porous plug carry an electric charge, an electrical double layer will be developed at the solid–liquid interface. The counterions are moved by the electric field, and, as they move, they pull the liquid in which they are embedded along with them. The volume of liquid transported per unit time by a known electric field can be used for the calculation of  $\zeta$ -potential. The conversion of the electroosmotic data depends on the system used in electroosmosis (i.e., single or narrow capillaries or porous plugs).

## Flow in Single Capillaries

For experiments conducted in capillaries of the usual size ( $10^{-3} < r < 10^{-1}$  cm), the electrical double layer is very thin compared to the capillary radius ( $\kappa r \gg 1$ ), and so the capillary surface may be regarded as flat. Therefore, the theory first given in its present form by Smoluchowski

may be applied in this case (11). According to this theory, the liquid moves adjacent to a large, flat, charged surface, under the influence of an electric field applied parallel to the surface. As the net excess of counterions in the adjacent liquid moves under the influence of the applied field, they draw the liquid along with them. The slipping plane is a plane parallel to the solid surface at a short distance,  $\delta$ , from it. The velocity of the liquid in the direction parallel to the solid surface,  $v_z$ , rises from zero in the slipping plane to a maximum one,  $v_{eo}$ , at some distance from the solid surface, after which it remains constant (Fig. 3A).  $v_{eo}$  is called electroosmotic velocity of the liquid. Note that contrary to the velocity of the liquid, electrostatic potential falls from  $\zeta$  to zero as we move away from the slipping plane.

Fig. 3B shows the forces exerted on a lamina of liquid of area  $A$  being in the diffuse part of the electrical double layer and containing a net countercharge,  $q$ , where  $q = \rho(x)Adx$ , under the influence of an electric field,  $E_z$ . The electrical force,  $F_q$ , is opposed by the net frictional force, which equals the balance between the frictional forces,  $F_1$

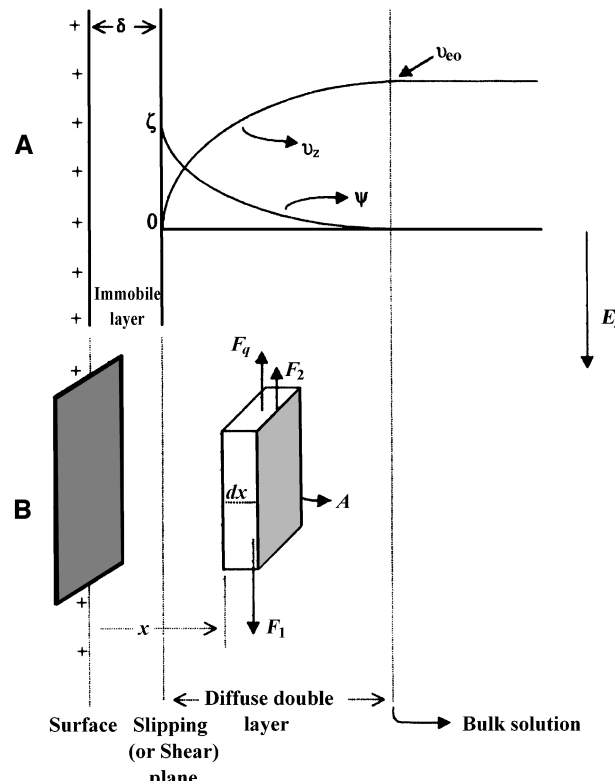


**Fig. 3** Variation of liquid velocity,  $v_z$ , and electrostatic potential,  $\psi$ , with the distance from the slipping plane (A) and forces exerted on an element of liquid volume of area  $A$  and net countercharge  $q$ .

and  $F_2$ , exerted on the two sides of the lamina of liquid. Consequently:

$$F_q = E_z q = F_1 - F_2$$

or

$$E_z q = E_z \rho(x) A d(x) = \eta A \left( \frac{dv_z}{dx} \right)_x - \eta A \left( \frac{dv_z}{dx} \right)_{x+dx}$$

or

$$E_z \rho(x) dx = -\eta \frac{d^2 v_z}{dx^2} dx \quad (10)$$

Substitution of  $\rho(x)$  from Poisson equation gives

$$E_z \epsilon \epsilon_0 \frac{d^2 \psi}{dx^2} dx = \eta \frac{d^2 v_z}{dx^2} dx \quad (11)$$

Eq. 11 can be integrated twice. First, it is integrated from a point far from the surface (i.e., in the bulk solution), where  $\psi = 0$  and  $v_z = v_{eo}$  (Fig. 3A), and therefore, both  $d\psi/dx$  and  $dv_z/dx$  are zero, up to a point in the double layer:

$$E_z \epsilon \epsilon_0 \frac{d\psi}{dx} = \eta \frac{dv_z}{dx}$$

The second integration takes place from a point again in the bulk solution to a point at the slipping plane where  $\psi = \zeta$  and  $v_z = 0$ :

$$-E_z \epsilon \epsilon_0 \zeta = \eta v_{eo}$$

or

$$v_{eo}/E_z = u_{eo} = -\epsilon \epsilon_0 \zeta / \eta \quad (12)$$

The integrations of Eq. 11 were done by assuming that both  $\epsilon$  and  $\eta$  retain their bulk values all through the double layer. The quantity  $u_{eo}$  is called electro-osmotic mobility in accordance with the electrophoretic mobility in electrophoresis (Eq. 1). The minus sign of Eq. 12 means that  $v_{eo}$  and  $E_z$  are either in the same direction when  $\zeta$  is negative or in opposite directions when  $\zeta$  is positive, as it is illustrated in Fig. 3, where the surface has been assumed to be positively charged. It should be noted that because no assumption was done for the distribution of charge or potential in the layer being between the solid surface and the slipping plane during the derivation of Eq. 12, the result (i.e., Eq. 12) is unaffected by the details of the charge arrangement in that layer. The only

assumption needed is that there is no movement of the liquid or of the charge inside that layer.

In practice, instead of  $v_{eo}$ , usually the electroosmotic volume flow,  $V_{eo}$ , which is the total volume of liquid that is transported through the capillary in unit time, is measured. As mentioned in the beginning of this section, the electrical double layer is very thin compared to the capillary radius ( $\kappa r \gg 1$ ). Provided that the region of varying velocity extends only through the double layer (Fig. 3A), it should be inferred that the liquid near the surface appears to move with the same velocity as that in the bulk solution. This type of flow is called plug flow. The profile of the liquid velocity across the capillary is shown in Fig. 4A. The electro-osmotic volume flow is then given by

$$V_{eo} = \pi r^2 v_{eo} = \pi r^2 \epsilon \epsilon_0 \zeta E_z / \eta \quad (13)$$

To eliminate the radius of the capillary (which may not be accurately known), we modify Eq. 13 by introducing the electric current,  $I$ , transported by the liquid:

$$\frac{I}{E_z} = \pi r^2 K^L \quad (14)$$

where  $K^L$  is the electrical conductivity of the bulk liquid (in ohm<sup>-1</sup> m<sup>-1</sup> or CV<sup>-1</sup>s<sup>-1</sup>m<sup>-1</sup>). Replacing  $E_z$  from Eq. 14, Eq. 13 yields

$$\frac{V_{eo}}{I} = \frac{\epsilon \epsilon_0 \zeta}{\eta K^L} \quad (15)$$

Eq. 15 is valid only if all, or almost all, of the current is carried through the bulk liquid. This is really the case if the electrolyte concentration is high. On the contrary, at low electrolyte concentration, the electric current due to the excess concentration of the counterions in the double layer is significant compared with that carried through the bulk liquid, and, therefore, it should be taken into account in the introduction of the electric current in the present analysis. So, at low electrolyte concentration, Eq. 14 must be replaced by

$$\frac{I}{E_z} = \pi r^2 K^L + 2\pi r K^\sigma = \pi r^2 \left( K^L + \frac{2K^\sigma}{r} \right) \quad (16)$$

where  $K^\sigma$  is the surface conductivity (in ohm<sup>-1</sup> or CV<sup>-1</sup>s<sup>-1</sup>).  $K^L$  and  $K^\sigma$  are multiplied by the cross-sectional area and circumference of the capillary, respectively, because  $K^L$  refers to the conductance of a cylindrical block of liquid of unit cross-sectional area and unit length, whereas  $K^\sigma$  refers to the conductance of a square sheet of

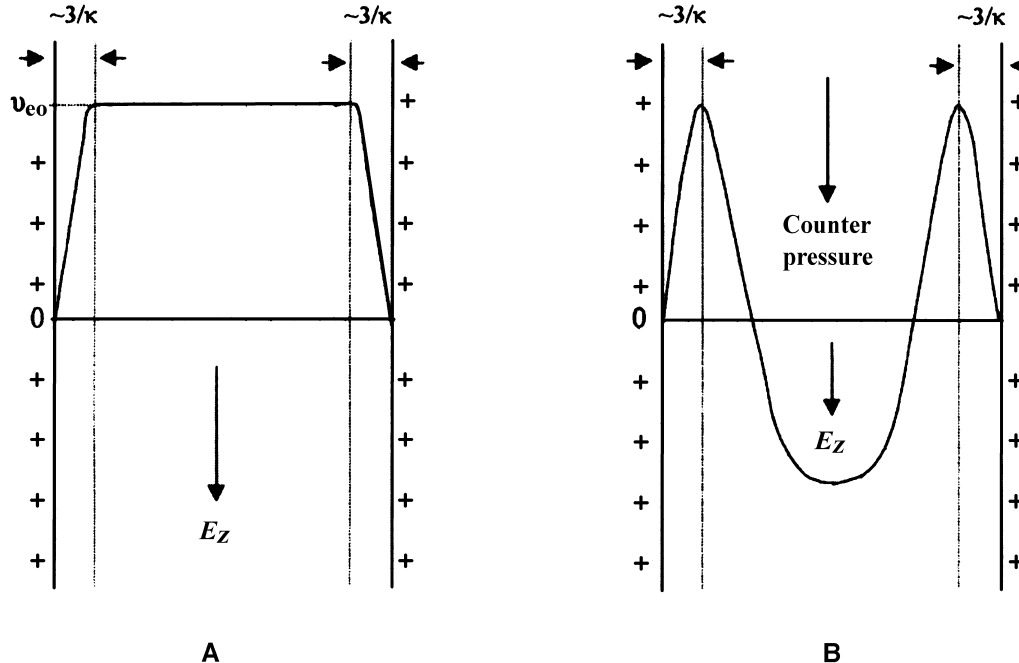


**Fig. 4** Profile of the liquid velocity in a capillary during (A) open tube electro-osmosis and (B) electroosmotic counter pressure measurement or closed tube electro-osmosis. The thickness of the double layer has been greatly exaggerated.

material of unit area and negligible thickness, measured along the length of the square. Eq. 15 is now transformed into

$$\frac{V_{eo}}{I} = \frac{\varepsilon \varepsilon_0 \zeta}{\eta \left( K^L + \frac{2K^\sigma}{r} \right)} \quad (17)$$

A more general form of the parenthesis is  $(K^L + fK^\sigma)$  where  $f$  is a “form factor” for the capillary, equal to the ratio of its circumference to its cross section (12, 13). Eq. 17 shows that the importance of the correction for surface conductance increases as  $r$  decreases and vanishes as  $r \rightarrow \infty$ . Eq. 17 also suggests that the values of the true  $\zeta$ -potential and  $K^\sigma$  may be determined by studying electro-osmosis in a set of capillaries identical in all respects except for varying radius. If the surface conductance is ignored, the variation of the determined  $\zeta$ -potential with the electrolyte concentration,  $\zeta(c)$ , exhibits a maximum in absolute value at low concentrations (12). This maximum is spurious for a surface with constant charge, such as the capillary surface. The spurious maximum comes from the fact that, as already mentioned, at low concentrations, the contribution of surface conductance is significant and should be taken into account. Otherwise, the elimination of the second term of

the parenthesis of Eq. 17 results in underestimated  $\zeta$ -potentials.

#### Electroosmotic counter pressure

The main problem of electroosmosis is the error that can result from the movement of the meniscus in the observation capillary (7). An alternative is the measurement of the applied on the fluid pressure,  $\Delta P_{eo}$ , required to create a Poiseuille flow just counterbalancing the electroosmotic one. Profile of the liquid velocity across the capillary is shown in Fig. 4B. The counterbalancing flow is given by Poiseuille equation, so for a capillary of length  $l$ :

$$V_{Pois.} = \frac{\pi r^4 \Delta P_{eo}}{8\eta l} = V_{eo} = \frac{\varepsilon \varepsilon_0 \zeta I}{\eta K^L}$$

Hence

$$\Delta P_{eo} = \frac{8\varepsilon \varepsilon_0 l \zeta I}{\pi r^4 K^L} \quad (18a)$$

Eq. 18a may be applicable also at low concentrations for single capillaries after a small modification, by taking into account surface conductance:

$$\Delta P_{eo} = \frac{8\varepsilon \varepsilon_0 l \zeta I}{\pi r^4 K^L + 2\pi r^3 K^\sigma} \quad (18b)$$

Unlike electroosmotic volume flow,  $\Delta P_{eo}$  may accurately be measured by means of accurate pressure transducers. It is therefore possible to overcome the errors introduced in the measurement of  $V_{eo}$ , by using the method of electro-osmotic counter pressure in single capillaries.

### Flow in Narrow Capillaries

The aforementioned considerations for the electroosmotic flow in single capillaries were made assuming  $\kappa r \gg 1$ , which means that the surface of the capillary, in a small area, may be considered as flat. On the other hand, the double layer is developed fully so that the electrostatic potential in the middle of the capillary (bulk solution) is zero (Fig. 3A). In narrow capillaries, double-layer overlap takes place. As a result, the potential in the middle of the capillary is non-zero. Moreover, the surface of the capillary may be regarded as flat only in the slit-shaped capillaries, whereas in the cylindrical narrow capillaries, the surface may not be regarded as flat. In this case, the cylindrical form of the Poisson-Boltzmann equation should be used for the description of the potential profile,  $\psi(x)$ . Next, the basic equations describing electro-osmosis in slit-shaped and cylindrical narrow capillaries shall be given. The calculation of  $\zeta$ -potential from electro-osmotic data is possible using these equations.

#### Slit-shaped capillaries

In a more complete analysis, the force exerted on the slab of the liquid illustrated in Fig. 3B, caused by any pressure gradient,

$$-\frac{dP}{dz}$$

should also be taken into account. The pressure gradient may be externally applied, or it may be developed along the capillary as a consequence of the electro-osmotic flow, if the flow is impeded. Eq. 11 should therefore be replaced by (12)

$$\varepsilon\epsilon_0 E_z \frac{d^2\psi}{dx^2} + \eta \frac{d^2v_z}{dx^2} - \frac{dP}{dz} = 0 \quad (19)$$

After the appropriate integrations, the mean fluid velocity was found to be

$$\bar{v} = \frac{h^2}{3\eta} \frac{dP}{dz} + \frac{\varepsilon\epsilon_0}{\eta} E_z \zeta [1 - G(z\zeta, \kappa h)] \quad (20)$$

where  $2h$  is the capillary width and  $G$  is a correction function defined by Burgreen and Nakache (14) as:

$$G(\zeta, \kappa h) = \frac{1}{h\zeta} \int_h^0 \psi(x) dx \quad (21)$$

For small potentials,  $\psi(x)$  may be expressed analytically (Ref. 11, p. 249), and the integral of Eq. 21 may thus be calculated. Consequently, the correction factor  $G$  may be derived analytically for low  $\zeta$ -potential:

$$G = \frac{\tan h\kappa h}{\kappa h} \quad (22)$$

Exactly calculated values of  $G$  as a function of  $\kappa h$  for various values of  $\zeta$  are illustrated by Hildreth (15). As shown, Eq. 22 is valid only for small values of  $\zeta$ -potential ( $ze\zeta/kT \leq 1$ ). At higher  $\zeta$  potentials, the true values of  $G$  are smaller than those calculated from Eq. 22 especially at small  $\kappa h$  values. A correction of the classical theory (i.e., Eq. 11) therefore is more likely for small values of  $\zeta$ -potential where larger values of the correction factor  $G$  are calculated according to Eq. 22.

For low potential values, Eq. 22 predicts values for  $G$  smaller than 0.05 for values of  $\kappa h$  greater than 18. Provided that in distilled water the value of  $\kappa$  is of the order of  $3 \times 10^4 \text{ cm}^{-1}$ , no significant correction of the classical theory is required for values of capillary width  $> 6 \mu\text{m}$ . The threshold of the capillary width, above which it is not necessary to modify Eq. 11, may be reduced even more for higher electrolyte concentrations or for higher  $\zeta$ -potentials. However, in the case of flow through oriented plates of clays, the corrections mentioned in this section seem to be necessary (12).

#### Cylindrical capillaries

As already mentioned in this case, the electrostatic potential profile is described by the Poisson-Boltzmann equation in cylindrical coordinates, which for a symmetrical electrolyte reads (Ref. 12, p. 32)

$$\frac{1}{y} \frac{d}{dy} \left( y \frac{d\psi}{dy} \right) = \frac{\kappa^2 kT}{ze} \sin h(ze\psi/kT) \quad (23)$$

where  $y$  is measured from the capillary axis. For low potentials Eq. 23 may be linearized by setting  $\sin h(ze\psi/kT) = ze\psi/kT$ :

$$\frac{1}{y} \frac{d}{dy} \left( y \frac{d\psi}{dy} \right) = \kappa^2 \psi \quad (24)$$

The solution of this equation by assuming that at  $y = r$  and  $\psi = \zeta$  yields:

$$\psi = \zeta \frac{I_0(\kappa y)}{I_0(\kappa r)} \quad (25)$$

where  $I_0$  is the Bessel function of first kind and of zero order.

Rice and Whitehead (16) solved the equation describing the flow of the liquid in the capillary by using Eq. 25 for the electrostatic potential profile and found that the electro-osmotic volume flow is given by Eq. 13, the right-hand side of which must be multiplied by the correction factor:

$$F(\kappa r) = 1 - \frac{2I_1(\kappa r)}{\kappa r I_0(\kappa r)} \quad (26)$$

where  $I_1$  is the Bessel function of first kind and of first order. Values of the correction factor  $F(\kappa r)$  as a function of  $\kappa r$  may also be found in Ref. 16. Consequently, the electro-osmotic volume flow is given by

$$V_{eo} = (\varepsilon \varepsilon_0 \pi r^2 \zeta E_z / \eta) F(\kappa r) \quad (27)$$

### Flow in Porous Plugs

For a plug of arbitrary geometry, Smoluchowski (11) has shown that Eq. 12 is still valid provided the pore diameter is much larger than  $\kappa^{-1}$ . Additionally, in the case of high electrolyte concentrations, where the contribution of surface conduction is negligible, Eqs. 15 and 18a, which have been derived from Eq. 12, are also valid. The flow of the liquid must be linear and laminar, a condition that is probably always satisfied in the experiments of electroosmosis.

However, porous plugs, as they are usually used in practical measurements, contain irregularly stacked heterogeneous particles forming unknown arrays with small pore size. It is not possible to develop a rigorous theory in such systems because of their complexity (13). Substantial simplifications are therefore needed. Two types of geometrical shapes may be elaborated: cylinder model and cell model. In the cylinder model, the plug or membrane can be considered to be composed of a collection of parallel tubes of given average radius,  $\langle r \rangle$ . In cell models, the porous system is considered to consist of granular material with usually homodispersed spherical particles, organized into a three-dimensional array.

Concerning the cylinder model, it is obvious that the analysis for narrow capillaries can readily be extended to describe it (16). On the other hand, O'Brien (17), based on the cell model, studied theoretically the electroosmosis in

a porous material composed of closely packed spheres immersed in a general electrolyte. A formula was obtained for the electro-osmotic flow rate in the case when the double layer is much thinner than the particle radius,  $a$  (i.e.,  $\kappa a \gg 1$ ):

$$\langle v \rangle = -\frac{\varepsilon \varepsilon_0 RT}{\eta F} \left\{ \frac{F\zeta}{RT} [1 + 3\varphi f(0)] - \left[ \frac{F\zeta}{RT} - \frac{2}{z} \ln 2 \right] g(Du) \right\} \langle E \rangle \quad (28)$$

where  $\langle v \rangle$  is the average of the local fluid velocity,  $v$ , over the plug cross section.  $\langle v \rangle$  is macroscopically identical with the electro-osmotic velocity ( $v_{eo}$ ).  $\langle E \rangle$  denotes the applied electric field. The explanation of the other symbols of Eq. 28 as well as its application to electrokinetic data for the calculation of  $\zeta$  will be discussed in detail that follows in the examination of streaming potential, because some investigators did not in fact measure electroosmotic velocity. A related quantity, the streaming potential or streaming current, is measured instead (18–20).

### STREAMING POTENTIAL

Streaming potential is the potential developed between the ends of a capillary, membrane, or porous plug when a liquid is forced under a hydrostatic pressure through them. The streaming potential is related to transfer of charge and mass occurring simultaneously by a number of mechanisms. As already mentioned, in electroosmosis, the surface of the capillary tube, of the membrane, and of the solid particles constituting the porous plug carry electric charge. An electrical double layer is thus developed at the solid–liquid interface. Applying pressure, the liquid moves and carries along with it the net charge, located in the mobile part of the double layer (i.e., in the diffuse part of the double layer). As a result, a steady convection current of double-layer ions is developed. Because this current arises under the influence of the flow of liquid in the absence of electric potential difference, it is called streaming current,  $I_s$ . The transport of ions by the streaming current results in the accumulation of charges of opposite sign at the ends of the capillary. As a result, an electric potential difference along the capillary develops. This potential difference opposes the mechanical transfer of the net charge by causing back movement of ions by electromigration (i.e., by conduction due to the ionic mobilities) and, to a much lesser extent, by electroosmotic flow. The transfer of charge due to these two effects is called the leak current (21). Because the potential

difference and, thus, the leak current increase as the charges accumulate at the ends of the capillary, soon after the application of the pressure gradient, the leak current reaches a value equal to that of the electric current due to convection (streaming current). A stationary state is therefore established, where no net current exists because streaming current and leak current cancel one another. Moreover, the potential difference between the ends of the capillary takes a maximum stationary value, called streaming potential,  $E_s$ . This potential must be measured, as a function of the applied pressure, with a very high impedance voltmeter (more than  $10^{11} \Omega$  input impedance), because the current withdrawn from the system needs to be practically zero (2). The measurement of streaming potential is an alternative method for the calculation of  $\zeta$ -potential. The relation between the streaming potential and the  $\zeta$ -potential depends on the systems used for the streaming potential measurement, which are the same as those used in electro-osmotic measurements (i.e., single or narrow capillaries or porous plugs).

### In Single Capillaries

The derivation of the classical equations relating streaming potential (or streaming current) with  $\zeta$ -potential is based on two important assumptions:

1. Laminar flow: This condition is easily fulfilled in practice because, in straight pipes, as the single capillaries are, turbulence occurs for Reynolds numbers equal to 2000 (12), a value that is high enough for streaming potential measurements.
2. The electrical double layer is very thin compared to

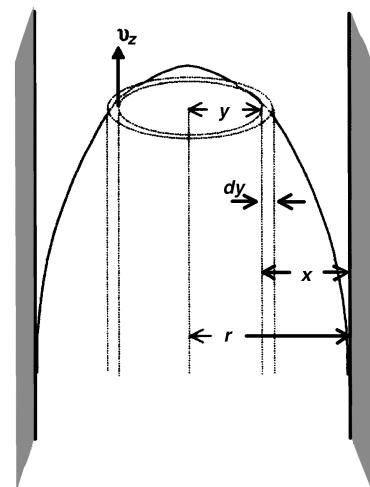


**Fig. 5** Liquid velocity profile in a capillary during a streaming potential measurement showing an elementary cylinder of liquid.

the capillary radius ( $kr \gg 1$ ), and so the capillary surface may be considered as flat.

Let  $P$  be the applied pressure difference at the ends of the capillary tube of radius,  $r$ , and length,  $l$ . As stated previously, the flow is laminar, and thus the liquid velocity at a distance  $y$  from the axis of the capillary (Fig. 5) is given by Poiseuille equation:

$$v_z(y) = P(r^2 - y^2)/4\eta l \quad (29)$$

Provided that the net charge carried by the moving liquid is confined to the double layer, that is to a thin region near the wall of the capillary, which means that the bulk of the moving liquid does not carry net charge, it may be inferred that only values of  $y$  near  $y = r$  are effective in determining the streaming current. Hence,  $y$  may be considered approximately equal to  $r$ , and consequently Eq. 29 may be transformed as follows (2):

$$v_z(y) \approx P(r - y)2r/4\eta l$$

or

$$v_z(x) \approx Prx/2\eta l \quad (30)$$

where  $x = r - y$  (Fig. 5).

The streaming current, which is the net charge carried by the moving liquid per unit time, is given by:

$$I_s = \int_0^r 2\pi y v_z(y) \rho(y) dy \quad (31)$$

or

$$I_s = - \int_r^0 2\pi(r - x) \frac{Prx}{2\eta l} \rho(x) dx \quad (32)$$

Because for the determination of  $I_s$  the effective values of  $x$  are confined to the double layer, they are negligible in comparison with the radius of the capillary. So  $r - x \approx r$  and Eq. 32 yields

$$I_s \approx - \frac{\pi r^2 P}{\eta l} \int_r^0 x \rho(x) dx \quad (33)$$

Substitution of  $\rho(x)$  from the Poisson equation and integration results in

$$\begin{aligned} I_s &= \frac{\pi r^2 P}{\eta l} \int_r^0 x \epsilon \epsilon_0 \frac{d^2 \psi}{dx^2} dx \\ &= \frac{\pi r^2 P \epsilon \epsilon_0}{\eta l} \left[ \left( x \frac{d\psi}{dx} \right)_{x=r}^{x=0} - \int_r^0 \frac{d\psi}{dx} dx \right] \\ &= - \frac{\pi r^2 P \epsilon \epsilon_0}{\eta l} \int_0^\zeta d\psi = - \frac{\epsilon \epsilon_0 \zeta}{\eta l} \pi r^2 P \end{aligned} \quad (34)$$

The first term in brackets is zero because the potential at  $x = r$  (and indeed long before  $x = r$ ) is zero, and so  $d\psi/dx$  is also zero.

Regarding the leak current, which is the current due to the motion of ions under the influence of the streaming potential, no significant error is introduced by assuming that the contribution of electro-osmosis is negligible. The entire backflow of ions therefore takes place exclusively by conduction. The conduction current,  $I_c$  is by definition given by Eq. 14, where the electric field strength,  $E_z$ , is related with the streaming potential,  $E_s$ , with  $E_z = E_s/l$ . So, Eq. 14 yields

$$I_c = \pi r^2 E_s K^L / l$$

When the steady state is established, the total current is zero; that is,  $I_s + I_c = 0$  and therefore

$$-\frac{\epsilon\epsilon_0\zeta\pi r^2 P}{\eta l} + \frac{\pi r^2 E_s K^L}{l} = 0$$

or

$$\frac{E_s}{P} = \frac{\epsilon\epsilon_0\zeta}{\eta K^L} \quad (35)$$

By comparing Eqs. 15 and 35, it may be observed that

$$\left(\frac{E_s}{P}\right)_{I=0} = \left(\frac{V_{eo}}{I}\right)_{P=0} \quad (36)$$

Eq. 36 is a fundamental relationship that has been found to be a direct consequence of Onsager's principle of reciprocity (12). This relationship suggests that electro-osmosis and streaming potential are too closely related electrokinetic phenomena, as may also be seen in Table 1. Table 1 shows that in electro-osmosis and streaming potential, the moving phase (liquid) and stationary phase (plug or capillary) are the same in both phenomena, whereas the driving force and the resulting phenomenon are reverse. Specifically, the driving force of electro-osmosis (streaming potential) is the applied electric field (pressure gradient), which in turn is the resulting phenomenon of streaming potential (electroosmosis).

Similarly with Eq. 15, Eq. 35 may be extended to the case of low electrolyte concentrations, where surface conduction is important. It may be done by replacing  $K^L$  with  $K^L + 2K^\sigma/r$ , so

$$\frac{E_s}{P} = \frac{\epsilon\epsilon_0\zeta}{\eta(K^L + \frac{2K^\sigma}{r})} \quad (37)$$

Comparison of Eqs. 17 and 37 shows that the fundamental Eq. 36 is valid even in systems involving surface conduction. As in electro-osmosis (Eq. 17), in streaming

potential measurements (Eq. 37), the true  $\zeta$ -potential and  $K^\sigma$  may be determined by measuring the streaming potential in a set of identical capillaries with varying radius. A simpler procedure of correcting for surface conduction is to multiply the right-hand side of Eq. 35 by the ratio  $R^c/R^\circ$  where  $R^c$  and  $R^\circ$  are the values of the resistance of the capillary corresponding to measurements with the under study electrolyte concentration and with high electrolyte concentration, where surface conduction is negligible (22). Eq. 35 then becomes

$$\frac{E_s}{P} = \frac{\epsilon\epsilon_0\zeta}{\eta K^L} \frac{R^c}{R^\circ} \quad (38)$$

### Streaming current measurements

At low electrolyte concentrations, more accurate values of  $\zeta$ -potential may be obtained by measuring streaming current instead of streaming potential. This is really the case because Eq. 34, which relates the streaming current with  $\zeta$ -potential, does not contain any conductivity term. It is therefore possible to avoid the effect of surface conduction, which at low electrolyte concentration is important and affects the streaming potential results. Moreover, the electric current involved is very small ( $\sim 10^{-10}$ – $10^{-11}$  A) at low electrolyte concentration (23), so that electrode polarization effects are negligible. At high electrolyte concentrations, however, where on one hand the effect of surface conduction vanishes and on the other hand the electric current is high enough so that the electrode polarization effect is appreciable, streaming potential is more convenient than streaming current for accurate measurements (24).

### In Narrow Capillaries

#### Slit-shaped capillaries

Hildreth (15) studied electrokinetic processes in slit-shaped capillaries and found a general expression for the electric current per unit area,  $I'$ :

$$I' = \frac{\epsilon\epsilon_0\zeta}{\eta l} (1 - G) P - \frac{K^c E}{l} \quad (39)$$

where  $G$  is the correction factor introduced first in section "Slit-shaped capillaries,"  $E$  is the developed potential difference due to the applied pressure gradient, and  $K^c$  is the conductivity of the liquid in the capillary, which may be measured independently in the absence of any pressure gradient. At the steady state, where  $E = E_s$ , the total current is zero ( $I' = 0$ ), so

$$\frac{E_s}{P} = \frac{\epsilon\epsilon_0\zeta}{\eta K^c} (1 - G) \quad (40)$$

The term  $1 - G$  is a correction related with the electric potential distribution (Eq. 21), so that the classical Eq. 35 is applicable in narrow capillaries. The use of  $K^c$  (Eq. 40) instead of  $K^L$  (Eq. 35) is necessary in order to take into account the effect of surface conduction.

### Cylindrical capillaries

As in electro-osmosis, in streaming potential, Rice and Whitehead (16) suggested the formula

$$\frac{E_s}{P} = \frac{\epsilon\epsilon_0\zeta}{\eta K^c} F(kr) \quad (41)$$

which is an extension of the classical Eq. 35 so that it is applicable in narrow cylindrical capillaries. The correction factor  $F(kr)$  given by Eq. 26, as stated in section "Cylindrical capillaries," is related with the potential distribution in cylindrical coordinates.  $K^c$  was used for the surface conduction effect to be included as in Eq. 40.

Because the analytical calculation of the potential profile (Eq. 25) and consequently the determination of  $F(kr)$  was obtained by assuming low potentials, Oldham et al. (25) tried to extend Eq. 41 to high potentials. They proposed an alternative expression for the correction factor  $F(kr, \zeta)$ , values of which as functions of  $kr$  and  $\zeta$  may be found in Ref. 7.

### In Porous Plugs

Prior to the theoretical idealizations, the practical alternative method elaborated by Briggs should be mentioned (22). According to this procedure,  $K^\sigma$  may be estimated as follows: The total conductance of the plug,  $G^*$ , is measured using first high electrolyte concentration (characterized by superscript "0"), where surface conduction is negligible and, therefore,  $G^{*,0} \approx G^{L,0}$ .  $G^{L,0}$  is the bulk conductance at the high concentration of electrolyte. The parameter relating the conductance ( $G$ ) to the conductivity ( $K$ ) of the plug, called cell constant of the plug, is then determined for the high electrolyte concentration, by the ratio  $G^{L,0}/K^{L,0}$  or  $G^{*,0}/K^{L,0}$ . The conductivity of plug due to the bulk electrolyte  $K^L$  may be easily measured at any electrolyte concentration ( $K^{L,0}$  and  $K^L$  for high and low concentrations, respectively). Because the cell constant of the plug is independent from the electrolyte concentration, it may be used to compute the conductivity of the plug ( $K^*$ ) from the respective total conductance of the plug ( $G^*$ ) measured at any electrolyte concentration:

$$K^* = G^*(K^{L,0}/G^{*,0}) \quad (42)$$

Finally,  $K^\sigma$  may be assessed by subtraction of  $K^L$  from  $K^*$ .

By substituting Eq. 42 for the classical Eq. 35, we obtain

$$\frac{E_s}{P} = \frac{\epsilon\epsilon_0\zeta}{\eta K^{L,0}} \frac{G^{*,0}}{G^*} \quad (43)$$

Provided that conductance is the reciprocal of resistance, Eqs. 43 and 38 are identical. Eq. 43 is a very good approximation as it follows from experimental results (7, 26). The spurious maximum shown by the variation of  $\zeta$ -potential calculated by using Eq. 35 with the electrolyte concentration,  $\zeta(c)$ , at low concentrations disappears when Eq. 43 is used, which is when the experimentally determined conductivity of the liquid in the plug (Eq. 42) is included.

Another procedure suggested by Chang and Robertson (12) especially for fibrous plugs results in

$$\frac{I_s \eta l}{\epsilon\epsilon_0 P} = -A\zeta \exp(-Bc) \quad (44)$$

where  $A$  is the cross-sectional area of the plug,  $B$  is a constant, and  $c$  is the concentration of the solid material in the plug, which is given by the ratio  $\phi/\beta$ .  $\phi$  and  $\beta$  are the volume fraction and the specific volume of the solid in the plug, respectively. It was observed that plots of  $\ln(I_s \eta l / \epsilon\epsilon_0 P)$  vs.  $c$  are quite linear for various fibrous plugs. The intercepts of these plots allow for the calculation of  $\zeta$ -potential. It is remarkable that although this procedure is empirical, the calculated potentials are in good agreement with those obtained by electrophoresis of small fibrous particles of the same material.

A considerable theoretical approach on the basis of the cell model was undertaken by O'Brien and Perrins (27). They derived a formula for the electrical conductivity of a porous plug composed of closely packed dielectric spheres in an electrolyte, by assuming the radius of the spheres,  $\alpha$ , to be much larger than the double-layer thickness ( $\kappa\alpha \gg 1$ ):

$$K^*/K^L = 1 + 3\phi \left[ f(0) + \left( K_2^L/K^L \right) (f(Du_2) - f(0)) \right] \quad (45)$$

where the subscript 2 refers to the counterions with the highest charge. The ratio  $K_2^L/K^L$  depends on the mobilities of the ions of the used electrolyte [e.g.,  $K_2^L/K^L$  equals 0.5 or 0.8 for KCl or HCl, respectively (27)].  $Du$  is a measure of the relative contribution of the surface conductance to the total conductance, given by the ratio  $K^\sigma/\alpha K^L$ . Except for symbol  $Du$ , introduced by Lyklema (Ref. 13, p. 3.208), other symbols (e.g.,  $\lambda$  or  $\beta$ ) are usually used in the electrokinetic literature by different authors to describe the contribution of surface conductance to the total one.

$f(Du)$  is a tabulated function of  $Du$  and of the type of packing of the particles in the plug (Table I of Ref. 27).  $Du_2$  is related to the  $\zeta$ -potential by (17, 19, 27)

$$Du_2 = (2/\kappa\alpha) \left[ 1 + \left( 3m_2/z_2^2 \right) + \Theta_2 \right] \times \left[ \exp(-z_2 e \zeta / 2kT) - 1 \right] \quad (46)$$

where  $m$  is a dimensionless parameter, accounting for the electroosmotic contribution to the surface conductivity, which for aqueous solutions at room temperature is 0.15 (13).  $\Theta$  represents the conduction behind the shear plane relative to the conduction due to electromigration beyond the shear plane (19).

A limiting expression of Eq. 45 may be obtained at sufficiently high ionic strength values, where the contribution of surface conductance is negligible ( $Du \ll 1$ ) (19, 20, 28):

$$K^* = (1 - 1.2\varphi)K^L + (2.4\varphi/\alpha)K^\sigma \quad (47)$$

The plug conductivity ( $K^*$ ) is calculated from the plug conductance ( $G^*$ ) and the cell constant based on the cell geometry or by means of Eq. 42. By plotting  $K^*$  vs.  $K^L$ , a straight line is obtained at relatively high ionic strength values, the slope and intercept of which allow for the determination of the particle volume fraction ( $\varphi$ ) and the surface conductivity ( $K^\sigma$ ) (19, 20, 28). Provided that the particle volume fraction is independent of the ionic strength, its value determined from the limiting Eq. 47 may be used in the general Eq. 45 to calculate the function  $f(Du_2)$  and consequently the value of  $Du_2$  (from Table I of Ref. 27), from conductivity measurements at any ionic strength. Assuming that the ions behind the shear plane are immobile ( $\Theta_2 = 0$ ),  $\zeta$ -potential may be calculated from  $Du_2$  using Eq. 46. In other words,  $\zeta$ -potential may be determined from conductivity measurements ( $\zeta^{\text{con}}$ ).

As already mentioned in section called "Flow in Porous Plug," O'Brien (17) suggested a formula for the velocity of a liquid that flows through a porous plug under the same assumptions as in the conductivity measurements (Eq. 28). Eq. 28 may easily be transformed into terms of streaming potential by using one of the Onsager's reciprocal relations (i.e., Eq. 36). The right-hand side of Eq. 36 may be replaced by the ratio  $\langle v \rangle / K^* \langle E \rangle$ , and by taking into account Eq. 28, we obtain (29)

$$\frac{E_s}{P} = \frac{1}{K^*} \frac{\varepsilon \varepsilon_0 R T}{\eta F} \left\{ \frac{F \zeta}{R T} [1 + 3\varphi f(0)] - \left[ \frac{F \zeta}{R T} - \frac{2}{z_1} \ln 2 \right] g(Du_2) \right\} \quad (48)$$

where  $z_1$  is the valence of the co-ion and  $g(Du)$  is a tabulated function of  $Du$  also depended on the type of packing of the particles in the plug (Table I of Ref. 17). If  $Du_2 \ll 1$  (sufficiently high ionic strengths),  $g(Du_2) \approx 0$  and the second term in Eq. 48 can be neglected, thus obtaining the Smoluchowski formula, which can be used for the calculation of  $\zeta$ -potential ( $\zeta^{\text{Smol}}$ ) (17):

$$\frac{E_s}{P} = - \frac{\varepsilon \varepsilon_0 \zeta (1 - 1.2\varphi)}{\eta K^*}$$

provided that  $f(0) \approx -0.4$  (Table 1 of Ref. 27).

A more thorough calculation of  $\zeta$ -potential is the application of the O'Brien theory (17) by assuming no conduction behind the shear plane ( $\Theta_2 = 0$ ).  $\zeta^{\Theta=0}$  is then estimated from  $Du_2$  (Eq. 46), which in turn may be calculated from streaming potential data (Eq. 48). Fig. 6 shows the variation of  $\zeta$ -potential obtained with different ways, as a function of ionic strength. A spurious maximum, which in the case of  $\zeta^{\Theta=0}$  is less pronounced, may be attributed to the fact that no conduction behind the shear plane was assumed. To the same reason should be ascribed the much higher values of  $\zeta^{\text{con}}$ .

Finally, an additional method for calculating  $\zeta$ -potential,  $\zeta^{\text{comb}}$ , is the combination of conductivity and streaming potential data using Eqs. 45 and 48 and assuming that the ions behind the shear plane are mobile ( $\Theta_2 \neq 0$ ). It may be observed in Fig. 6 that the spurious maximum disappears when surface conduction behind the shear plane is accounted for. The relative contribution of this kind of surface conduction,  $\Theta_2$ , may also be cal-

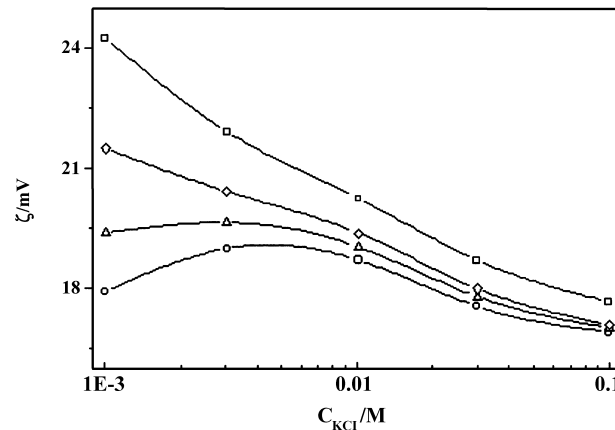


**Fig. 6** Variation with the electrolyte concentration of  $\zeta$ -potential calculated: 1) from conductivity measurements,  $\zeta^{\text{con}}$  ( $\square$ ), 2) according to Smoluchowski theory,  $\zeta^{\text{Smol}}$ , ( $\circ$ ), and 3) according to the O'Brien theory with  $\Theta = 0$ ,  $\zeta^{\Theta=0}$  ( $\triangle$ ) and  $\Theta \neq 0$ ,  $\zeta^{\text{comb}}$  ( $\diamond$ ). The plug was composed with titania particles doped with  $\text{Nb}^{5+}$ . (Unpublished results.)

culated in this way of interpretation of the electrokinetic results, when  $\zeta$  is already determined, by means of Eq. 46. Results similar to those illustrated in Fig. 6 have also been obtained by other investigators for various materials (e.g., Refs. 19 and 20).

### SEDIMENTATION POTENTIAL (DORN EFFECT)

When a charged colloidal particle is sedimenting through a liquid, the particle moves ahead of its ionic countercharge, thus creating an electric potential difference called sedimentation potential,  $E_{\text{sed}}$ . The so-created electric field,  $E_z$ , is parallel (or antiparallel) to the direction of the motion of the particles and is equal to  $E_{\text{sed}}/l$ , where  $l$  is the distance between the two electrodes measuring the potential difference. The measurement of  $E_{\text{sed}}$  allows for the determination of  $\zeta$ -potential.

An approximate relation between  $E_{\text{sed}}$  and  $\zeta$  for  $\kappa\alpha \ll 1$  may be derived, considering the sedimentation of  $N$  particles per unit volume of charge  $Q$  and radius  $\alpha$ , settling in a liquid medium with a velocity  $v_{\text{sed}}$ . The sedimentation of the particles causes an electric current in one direction, the density of which is equal to  $Nv_{\text{sed}}Q$ , whereas the ions moved under the influence of the sedimentation field cause a current in the opposite direction with a density equal to  $E_{\text{sed}}K^L/l$ .  $K^L$  is again the conductivity of the bulk ionic solution. In the steady state, the two electric currents are equal:

$$Nv_{\text{sed}}Q = E_{\text{sed}}K^L/l \quad (49)$$

Substituting for  $v_{\text{sed}}$  from Stoke's law  $v_{\text{sed}} = 2\alpha^2 g \Delta d / 9\eta$ , where  $\Delta d$  is the difference of densities between particle and the suspension medium and  $g$  is the standard acceleration of free fall, and replacing  $Q$  with  $4\pi\epsilon\epsilon_0\alpha\zeta$ , we obtain

$$E_{\text{sed}} = \frac{8\pi\epsilon\epsilon_0\zeta\alpha^3 g \Delta d N I}{9\eta K^L} \quad (50)$$

In the case of thin double layer ( $\kappa\alpha \gg 1$ ), Smoluchowski derived the following equation, ignoring the effect of surface conduction (12):

$$E_{\text{sed}} = \frac{4\pi\epsilon\epsilon_0\zeta\alpha^3 g \Delta d N I}{3\eta K^L} \quad (51)$$

The fact that Eqs. 50 and 51 differ by a factor 3/2 as do the corresponding limiting laws for electrophoresis (Eqs. 7 and 8) demonstrates that, as shown in the section entitled "In Single Capillaries" for electro-osmosis and

streaming potential, sedimentation potential and electrophoresis are very closely related electrokinetic phenomena. Indeed, as it may also be seen from Table 1, in electrophoresis and sedimentation potential, the moving phase (particles) and stationary phase (liquid) are the same in both phenomena, whereas the driving force and the resulting phenomenon are opposite. Specifically, the driving force of electrophoresis (sedimentation potential) is the applied electric field (particle movement), which in turn is the resulting phenomenon of sedimentation potential (electrophoresis). Results concerning intermediate  $\kappa\alpha$  values have been reported by Stigter and Ohshima and colleagues (30, 31).

In the case where the sedimenting particle is a fluid of finite viscosity (e.g., an emulsion droplet), the sedimentation velocity is given by a different equation than that for the solid particle (12):

$$v_{\text{sed}} = \frac{2\alpha^2 g \Delta d}{9\eta} \left[ \frac{3\eta + 3\eta' + \sigma_e^2/K^L}{2\eta + 3\eta' + \sigma_e^2/K^L} \right]$$

where  $\eta'$  is the viscosity of the fluid drop and  $\sigma_e$  is the charge density in the shear plane. The relation between  $E_{\text{sed}}$  and  $\zeta$  is then, in our notation, given by (12)

$$E_{\text{sed}} = \frac{4\pi\epsilon\epsilon_0\zeta\alpha^3 g \Delta d N I}{3K^L(2\eta + 3\eta' + \sigma_e^2/K^L)} \quad (52)$$

A critical question arising by finishing this article is whether the value of  $\zeta$ , obtained from one of the aforementioned electrokinetic techniques, is correct. This question cannot be directly answered because there is no independent way of measuring electrokinetic potentials. The only way to assess the quality of results obtained is to deduce  $\zeta$ -values from different electrokinetic techniques for a given material and solution and compare them. Provided that  $\zeta$ -potential is a material property, that is, determined only by the nature of the surface, its charge and the presence of adsorbates, properly analyzed different types of electrokinetics, should lead to similar  $\zeta$ -potential values.

### LIST OF SYMBOLS

*Latin:*

<i>A</i>	— surface area
<i>c</i>	— concentration
<i>d</i>	— particle density
<i>Du</i>	— relative surface conductance (or Dukhin number)

$e$	— elementary charge
$E$	— electric field strength
$E_s$	— streaming potential
$E_{\text{sed}}$	— sedimentation potential
$F$	— Faraday constant ( $\text{C mol}^{-1}$ )
$F_q$	— electrical force
$F_1, F_2$	— frictional forces
$g$	— standard acceleration of free fall
$G$	— conductance ( $\text{S}$ or $\text{C V}^{-1} \text{s}^{-1}$ )
$G$	— correction factor
$h$	— slit-shaped capillary width
$I$	— ionic strength
$I$	— electric current
$I_c$	— conduction current
$I_o$	— Bessel function of first kind and zero order
$I_1$	— Bessel function of first kind and first order
$I_s$	— streaming current
$I'$	— electric current per unit area
$k$	— Boltzmann's constant ( $\text{JK}^{-1}$ )
$K$	— conductivity ( $\text{S m}^{-1}$ or $\text{C V}^{-1} \text{m}^{-1} \text{s}^{-1}$ )
$K''$	— surface conductivity ( $\text{S}$ or $\text{C V}^{-1} \text{s}^{-1}$ )
$N$	— number of particles per unit volume
$N_A$	— Avogadro constant
$P$	— pressure difference
$P_{\text{eo}}$	— electroosmotic pressure
$q$	— electric countercharge
$Q$	— electric charge
$r$	— radius of capillary
$R$	— electric resistance
$R$	— gas constant ( $\text{J K}^{-1} \text{mol}^{-1}$ )
$\text{Rel}$	— measure of the surface conductivity and double-layer relaxation effect
$T$	— temperature (K)
$u$	— electrophoretic mobility
$u_{\text{eo}}$	— electroosmotic mobility
$v_{\text{sed}}$	— sedimentation velocity
$v_{\text{eo}}$	— electroosmotic velocity (or maximum velocity) of liquid
$v_z$	— velocity of liquid parallel to the surface of the solid
$\bar{v}$	— mean fluid velocity
$v$	— local fluid velocity
$V_{\text{eo}}$	— electroosmotic volume flow
$V_{\text{Pois}}$	— counterbalancing liquid flow
$z$	— valence

*Greek:*

$\alpha$	— particle radius
$\beta$	— specific solid volume ( $\text{m}^3 \text{Kg}^{-1}$ )
$\delta$	— distance between surface and slipping plane
$\epsilon$	— relative dielectric permittivity (dielectric constant)

**Calculation of Zeta-Potentials from Electrokinetic Data**

$\epsilon_0$	— dielectric permittivity of vacuum ( $\text{C}^2 \text{N}^{-1} \text{m}^2$ or $\text{C V}^{-1} \text{m}^{-1}$ )
$\zeta$	— electrostatic potential at the shear plane
$\eta$	— viscosity of the liquid
$\eta'$	— fluid drop viscosity
$\Theta$	— relative conduction behind the shear plane
$\kappa$	— reciprocal Debye length
$\lambda$	— conductivities' function
$\rho$	— electric charge density
$\phi$	— volume fraction of the solid in the plug
$\psi$	— electrostatic potential
$\psi_d$	— Stern potential

**REFERENCES**

- Shaw, D.J. Charged Interfaces. In *Introduction to Colloid and Surface Chemistry*, 3rd Ed.; Butterworths: London, 1985; 162.
- Hunter, R.J. Measuring Surface Charge and Potential. In *Introduction to Modern Colloid Science*, 1st Ed.; Oxford, Science Publications: New York, 1993; 227–261.
- Sugrue, S.; Oja, T.; Bott, S. In *Advances in Simultaneous, Multiangle Doppler Electrophoretic Light Scattering Analysis*; International Laboratory, May 1989; 34.
- McFadyen, P. In *Electrophoretic Mobility and Zeta Potential of Colloidal Particles*, International Laboratory, September 1986; 32.
- Hardware Reference Manual for MALVERN Zetasizer 5000*.
- Overbeek, J.Th.C.; Bijsterbosch, B.H. The Electrical Double Layer and the Theory of Electrophoresis. In *Electrokinetic Separation Methods*; Rigetti, P.G., van Oss, C.J., Vanderhoff, J.W., Eds.; Elsevier, 1979; 15.
- Dukhin, S.S.; Derjaguin, B.V. Equilibrium Double Layer and Electrokinetic Phenomena. In *Surface and Colloid Science*; Matijevic, E., Ed.; J. Wiley & Sons: New York, 1974; Vol. 7, 49–272.
- Ohshima, H.; Healy, W.T.; White, L.R. Approximate analytic expressions for the electrophoretic mobility of spherical colloidal particles and the conductivity of their dilute suspensions. *J. Chem. Soc. Faraday Trans. II* **1983**, 1613.
- Birdi, K.S. Chemical Physics of Colloid Systems and Interfaces. In *Handbook of Surface and Colloid Chemistry*, 1st Ed.; Birdi, K.S., Ed.; CRC Press: Boca Raton, 1997; 435.
- MALVERN Application Note: “Zeta potential in Pharmaceutical Formulation”.
- Overbeek, J.Th.G. Electrokinetic Phenomena. In *Colloid Science*; Kruijt, H.R., Ed.; Elsevier: Amsterdam, 1952; Vol. I, 194–244.
- Hunter, R.J. The Calculation of Zeta Potential. In *Zeta Potential in Colloid Science*; Ottewill, R.H., Rowell, R.L., Eds.; Academic Press: London, 1981; 59–124.

13. Lyklema, J. Electrokinetics and Related Phenomena. In *Fundamentals of Interface and Colloid Science* Academic Press: London, 1995; Vol. II, 4.1–4.135.
14. Burgreen, D.; Nakache, F.R. Electrokinetic flow in ultrafine capillary slits. *J. Phys. Chem.* **1964**, *68*, 1084–1091.
15. Hildreth, D. Electrokinetic flow in fine capillary channels. *J. Phys. Chem.* **1970**, *74*, 2006–2015.
16. Rice, C.L.; Whitehead, R. Electrokinetic flow in a narrow cylindrical capillary. *J. Phys. Chem.* **1965**, *69*, 4017–4023.
17. O'Brien, R.W. Electroosmosis in porous materials. *J. Colloid Interface Sci.* **1986**, *110*, 477–487.
18. van der Put, A.G.; Bijsterbosch, B.H. Electrokinetic measurements on concentrated polystyrene dispersions and their theoretical interpretation. *J. Colloid Interface Sci.* **1983**, *92*, 499–507.
19. Minor, M.; van der Linde, A.J.; Lyklema, J. Streaming potentials and conductivities of latex plugs in indifferent electrolytes. *J. Colloid Interface Sci.* **1998**, *203*, 177–188.
20. Minor, M.; van der Linde, A.J.; van Leeuwen, H.P.; Lyklema, J. Streaming potential and conductivities of porous silica plugs. *Colloids Surf.-A* **1998**, *142*, 165–173.
21. Shaw, D.J. Streaming Potential and Electroosmosis. In *Electrophoresis*; Academic Press: London, 1969; 76–84.
22. Briggs, T.R. The determination of the  $\zeta$ -potential on cellulose-a model. *J. Phys. Chem.* **1928**, *32*, 641–675.
23. Hurd, R.M.; Hackermann, N. Electrokinetic potentials of bulk metals by streaming-current measurements. *J. Electrochem. Soc.* **1955**, *102*, 594–597.
24. van der Linde, A.J.; Bijsterbosch, B.H. Electrode polarization and its implications in streaming potential and streaming current measurements. *Colloids Surf.* **1989**, *41*, 345–352.
25. Oldham, I.B.; Young, F.G.; Osterle, J.F. Streaming potential in small capillaries. *J. Colloid Sci.* **1963**, *18*, 328–336.
26. van der Linde, A.J.; Bijsterbosch, B.H. Does the maximum in the zeta potential of monodisperse polystyrene particles really exists? An electrokinetic study. *Croat. Chem. Acta* **1990**, *63*, 455–465.
27. O'Brien, R.W.; Perrins, W.T. The electrical conductivity of a porous plug. *J. Colloid Interface Sci.* **1984**, *99*, 20–31.
28. Spanos, N.; Tsevis, A.; Koutsoukos, P.G.; Minor, M.; van der Linde, A.J.; Lyklema, J. Electro-kinetic measurements on plugs of doped titania. *Colloids Surf.-A* **1998**, *141*, 101–109.
29. Spanos, N.; Koutsoukos, P.G. Calculations of zeta potential from electrokinetic measurements on titania plugs. *J. Colloid Interface Sci.* **1999**, *214*, 85–90.
30. Stigter, D. Sedimentation of highly charged colloid spheres. *J. Phys. Chem.* **1980**, *84*, 2758–2762.
31. Ohshima, H.; Healy, T.W.; O'Brien, R.W.; White, L.R. Sedimentation-velocity and potential in a dilute suspension of charged spherical colloidal particles. *J. Chem. Soc., Faraday Trans. II* **1984**, *80*, 1299–1317.